

## THE INFLUENCE OF MATERIAL PROPERTIES ON THE $Q$ -STRESS VALUE NEAR THE CRACK TIP FOR ELASTIC-PLASTIC MATERIALS

MARCIN GRABA

*Kielce University of Technology, Faculty of Mechatronics and Machine Design, Kielce, Poland  
e-mail: mgraba@tu.kielce.pl*

In the paper, the values of the  $Q$ -stress determined for various elastic-plastic materials for single edge notched specimens in bending (SEN(B)) are presented. The influence of the yield strength, the work-hardening exponent and the crack length on the  $Q$ -parameter is tested. The numerical results are approximated by closed form formulas.

*Key words:*  $Q$ -stress,  $J$ - $Q$  theory, fracture mechanics

### 1. Introduction

In 1968 J.W. Hutchinson (Hutchinson, 1968) published a fundamental work, which characterized stress fields in front of a crack for the non-linear Ramberg-Osgood (R-O) material in the form

$$\sigma_{ij} = \sigma_0 \left( \frac{J}{\alpha \sigma_0 \varepsilon_0 I_n r} \right)^{\frac{1}{1+n}} \tilde{\sigma}_{ij}(\theta, n) \quad (1.1)$$

where  $r$  and  $\theta$  are polar coordinates of the coordinate system located at the crack tip,  $\sigma_{ij}$  are components of the stress tensor,  $J$  is the  $J$ -integral,  $n$  – R-O exponent,  $\alpha$  – R-O constant,  $\sigma_0$  – yield stress,  $\varepsilon_0$  – strain related to  $\sigma_0$  through  $\varepsilon_0 = \sigma_0/E$ . The functions  $\tilde{\sigma}_{ij}(n, \theta)$ ,  $I_n(n)$  must be found by solving the fourth order non-linear homogenous differential equation independently for the plane stress and plane strain (Hutchinson, 1968). Equation (1.1) is commonly called the "HRR solution".

The HRR solution includes the first term of the infinite series only. The numerical analysis shows that results obtained using the HRR solution are different from the results obtained by the finite element method (FEM). To eliminate this difference, it is necessary to use more terms in the HRR solution.

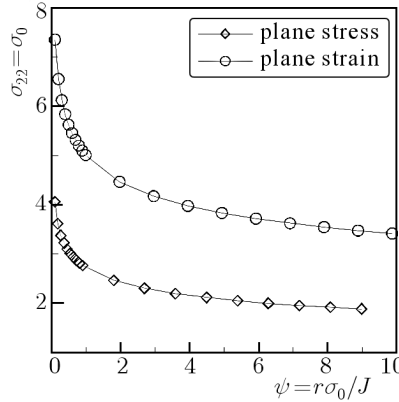


Fig. 1. The crack opening stress distribution for elastic-plastic materials, obtained using the HRR solution (own calculation);  $E = 206000$  MPa,  $n = 5$ ,  $\sigma_0 = 315$  MPa,  $\nu = 0.3$ ,  $\varepsilon_0 = 0.00153$ ,  $\theta = 0$

Li and Wang (1985) using two terms in the Airy function obtained the second term of the asymptotic expansion for the two materials described by  $n = 3$  and  $n = 10$ . Next, they compared their results with the HRR fields and FEM results. Their analysis showed that using the two term solution to describe the stress field near the crack tip brings closer analytical results to the FEM results. Two term solution much better describes the stress field near the crack tip, and the value of the second term, which may not be negligible depending on the material properties and geometry of the specimen.

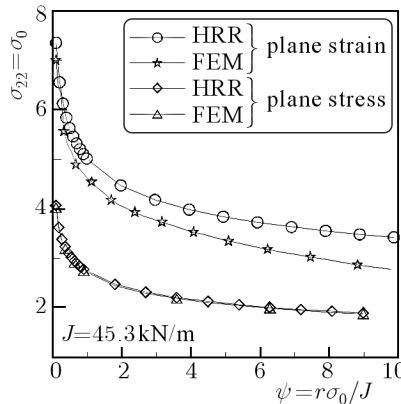


Fig. 2. A comparison of the FEM results and HRR solution for plane stress and plane strain for a single edge notched specimen under bending (SEN(B)) (own calculation);  $a/W = 0.5$ ,  $W = 40$  mm,  $E = 206000$  MPa,  $n = 5$ ,  $\sigma_0 = 315$  MPa,  $\nu = 0.3$ ,  $\varepsilon_0 = 0.00153$ ,  $\theta = 0$

Yang *et al.* (1993) using the Airy function with the separate variables in the infinite series form, proposed that the stress field near the crack tip may be described by Eq. (1.2) in an infinite series form

$$\frac{\sigma_{ij}}{\sigma_0} = \sum_{k=1}^{+\infty} A_k \bar{r}^{s_k} \tilde{\sigma}_{ij}^{(k)}(\theta) \quad (1.2)$$

where  $k$  is the number of series terms,  $A_k$  is the amplitude for the  $k$ -th series term,  $\bar{r}$  is the normalized distance from the crack tip,  $s_k$  is the power exponent for the  $k$ -th series term, and  $\tilde{\sigma}_{ij}^{(k)}$  is the "stress" function.

When limited to three terms only, Eq. (1.2) may be written in the following form

$$\frac{\sigma_{ij}}{\sigma_0} = A_1 \bar{r}^s \tilde{\sigma}_{ij}^{(1)}(\theta) + A_2 \bar{r}^t \tilde{\sigma}_{ij}^{(2)}(\theta) + \frac{A_2^2}{A_1} \bar{r}^{2t-s} \tilde{\sigma}_{ij}^{(3)}(\theta) \quad (1.3)$$

where the  $\tilde{\sigma}_{ij}^{(k)}$  functions must be found by solving the fourth order non-linear homogenous differential equation independently for the plane stress and plane strain (Yang *et al.*, 1993),  $s$  is the power exponent, which is identical to one in the HRR solution ( $s$  may be calculated as  $s = -1/(n+1)$ ),  $t$  is the power exponent for the second term of the asymptotic expansion, which must be found numerically by solving the fourth order non-linear homogenous differential equation independently for the plane stress and plane strain (Yang *et al.*, 1993),  $\bar{r}$  is the normalized term of the asymptotic expansion, which must be found numerically by solving the fourth order non-linear homogenous differential equation independently for the plane stress and plane strain (Yang *et al.*, 1993),  $\bar{r}$  is the normalized distance from the crack tip calculated as  $\bar{r} = r/(J/\sigma_0)$ ,  $A_1$  is the amplitude of the first term of the infinite series evaluated as  $A_1 = 1/(\alpha \varepsilon_0 I_n)^{n+1}$ , and  $A_2$  is the amplitude of the second term, which is calculated by fitting Eq. (1.3) to the numerical results of the stress fields close to the crack tip.

Shih *et al.* (1993) proposed a simplified solution. They assumed that the FEM results are exact and computed the difference between the numerical and HRR results. They proposed that the stress field near the crack tip may be described by the following equation

$$\frac{\sigma_{ij}}{\sigma_0} = \left( \frac{J}{\alpha \varepsilon_0 \sigma_0 I_n r} \right)^{\frac{1}{n+1}} \tilde{\sigma}_{ij}(\theta, n) + Q \left( \frac{r}{J/\sigma_0} \right)^q \hat{\sigma}_{ij}(\theta, n) \quad (1.4)$$

where  $\hat{\sigma}_{ij}(\theta, n)$  are functions evaluated numerically,  $q$  is the power exponent, whose value changes in the range (0, 0.071), and  $Q$  is a parameter, which is the amplitude of the second term in the asymptotic solution.

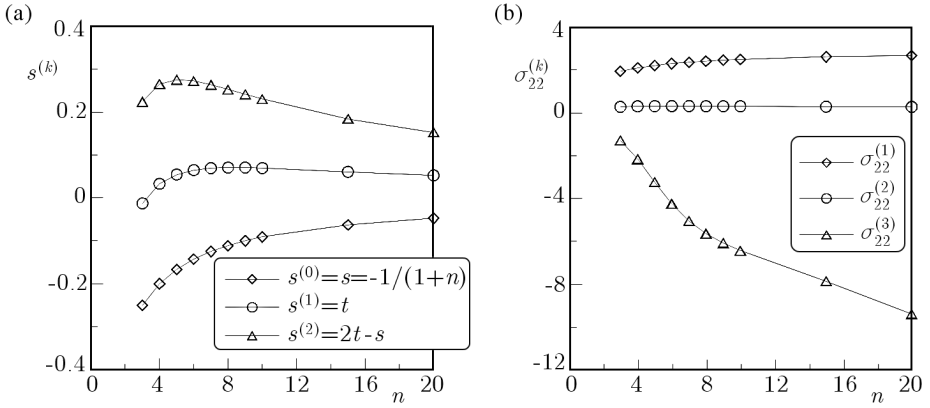


Fig. 3. The influence of the work hardening exponent on the power exponents  $s^{(k)}$  (a) and the "stress" functions  $\tilde{\sigma}_{ij}^{(k)}$  (b) for three terms of the asymptotic solution (own graphs based on results presented in Yang *et al.* (1993))

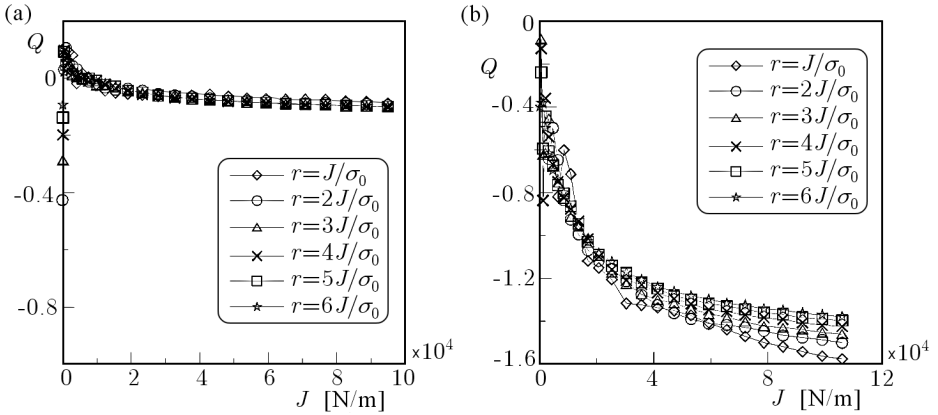


Fig. 4.  $J$ - $Q$  trajectories for a centrally cracked plate under tension (CC(T)): (a) plane stress; (b) plane strain (own calculation);  $W = 40$  mm,  $a/W = 0.5$ ,  $\sigma_0 = 315$  MPa,  $\nu = 0.3$ ,  $E = 206000$  MPa,  $n = 5$

O'Dowd and Shih (1991, 1992) tested the  $Q$ -parameter in the range  $J/\sigma_0 < r < 5J/\sigma_0$  near the crack tip. They showed that the  $Q$ -parameter weakly depends on the crack tip distance in the range of the  $\pm\pi/2$  angle. O'Dowd and Shih proposed only two terms to describe the stress field near the crack tip

$$\sigma_{ij} = (\sigma_{ij})_{HRR} + Q\sigma_0\hat{\sigma}_{ij}(\theta) \tag{1.5}$$

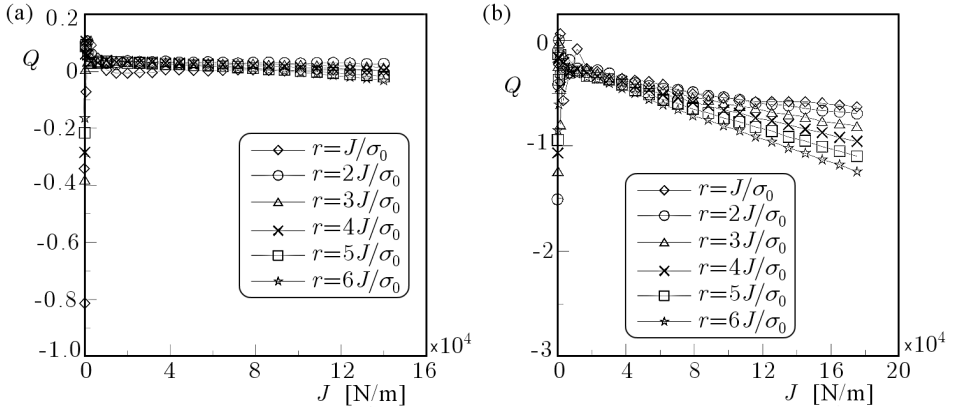


Fig. 5.  $J$ - $Q$  trajectories for a single edge notched specimen under bending (SEN(B)): (a) plane stress; (b) plane strain (own calculation);  $W = 40$  mm,  $a/W = 0.5$ ,  $\sigma_0 = 315$  MPa,  $\nu = 0.3$ ,  $E = 206000$  MPa,  $n = 5$

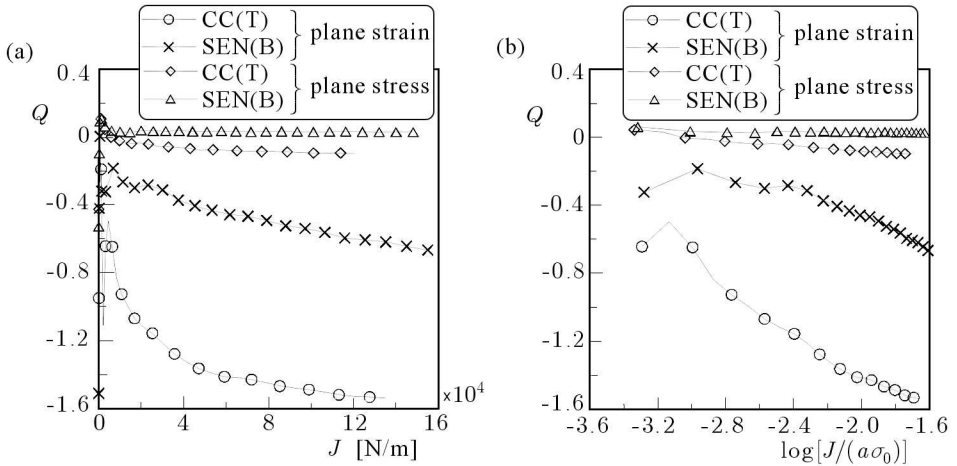


Fig. 6. A comparison of  $J$ - $Q$  trajectories (a) and  $Q = f(\log[J/(a\sigma_0)])$  trajectories (b) for CC(T) and SEN(B) specimen (own calculation);  $W = 40$  mm,  $a/W = 0.5$ ,  $\sigma_0 = 315$  MPa,  $\nu = 0.3$ ,  $E = 206000$  MPa,  $n = 5$ ,  $r = 2J/\sigma_0$

To avoid the ambiguity during the calculation of the  $Q$ -stress, O’Dowd and Shih suggested, where the  $Q$ -stress may be evaluated. It was assumed that the  $Q$ -stress should be computed at  $r = 2J/\sigma_0$  in the  $\theta = 0$  direction. O’Dowd and Shih postulated that for  $\theta = 0$  the function  $\hat{\sigma}_{\theta\theta}(\theta = 0)$  is equal to 1. That is why the  $Q$ -stress may be calculated from the following relationship

$$Q = \frac{(\sigma_{\theta\theta})_{FEM} - (\sigma_{\theta\theta})_{HRR}}{\sigma_0} \quad \text{for } \theta = 0 \quad \text{and} \quad \frac{r\sigma_0}{J} = 2 \quad (1.6)$$

where  $(\sigma_{\theta\theta})_{FEM}$  is the stress value calculated using FEM, and  $(\sigma_{\theta\theta})_{HRR}$  is the stress value evaluated from the HRR solution. During analysis, O'Dowd and Shih showed that in the range of  $\theta = \pm\pi/4$ , the following relationships take place:  $Q\hat{\sigma}_{\theta\theta} \approx Q\hat{\sigma}_{rr}$ ,  $\hat{\sigma}_{\theta\theta}/\hat{\sigma}_{rr} \approx 1$  and  $Q\hat{\sigma}_{r\theta} \approx 0$  (because  $Q\hat{\sigma}_{r\theta} \ll Q\hat{\sigma}_{\theta\theta}$ ). Thus, the  $Q$ -stress value determines the level of the hydrostatic stress. For the plane stress, the  $Q$ -parameter is equal to zero, but for the plane strain, the  $Q$ -parameter is, in most cases, smaller than zero.

## 2. Discussion about $J$ - $A_2$ and $J$ - $Q$ theory

To describe the stress field near the crack tip for elastic-plastic materials, the HRR solution is most often used, Eq. (1.1). However, the results obtained are usually overestimated and the analysis is conservative.

A lot of analyses, which were carried out in the nineties, proved that the multi-terms description using three terms of the asymptotic solution is better than O'Dowd's approach. The  $A_2$  amplitude, which is used in the  $J$ - $A_2$  theory suggested by Yang *et al.* (1993) is nearly independent of the distance of its determination in contrast to the  $Q$ -stress, which depends on the place where it is calculated. But the  $J$ - $A_2$  theory sometimes is very burdensome, because an engineer must solve a fourth order nonlinear differential equation to determine the  $\tilde{\sigma}_{ij}^{(k)}$  function and the power exponent  $t$ . Next, the engineer using FEM results calculates the  $A_2$  amplitude by fitting Eq. (1.3) to the numerical results.

For using the O'Dowd approach, the engineer needs the  $Q$ -stress only (calculated numerically). That is why the O'Dowd approach is easier and more convenient to use in contrast to the  $J$ - $A_2$  theory. The  $J$ - $Q$  theory found application in European Engineering Programs, like SINTAP or FITNET. The  $Q$ -stress is applied for formulation of the fracture criterion and to the assessment of the fracture toughness of the structural component. Thus the O'Dowd theory has practical application in engineering issues.

Sometimes, the application of the  $J$ - $Q$  theory may be limited, because there is no value of the  $Q$ -stress for a given material and specimen. Using any fracture criterion, for example proposed by O'Dowd (1995), or another criterion, the engineer can estimate the fracture toughness quite fast, if the  $Q$ -stress is known. The literature does not announce a  $Q$ -stress catalogue and  $Q$ -stress values as a function of the external load, material properties or geometry of the specimen. In some papers, the engineer may find  $J$ - $Q$  graphs

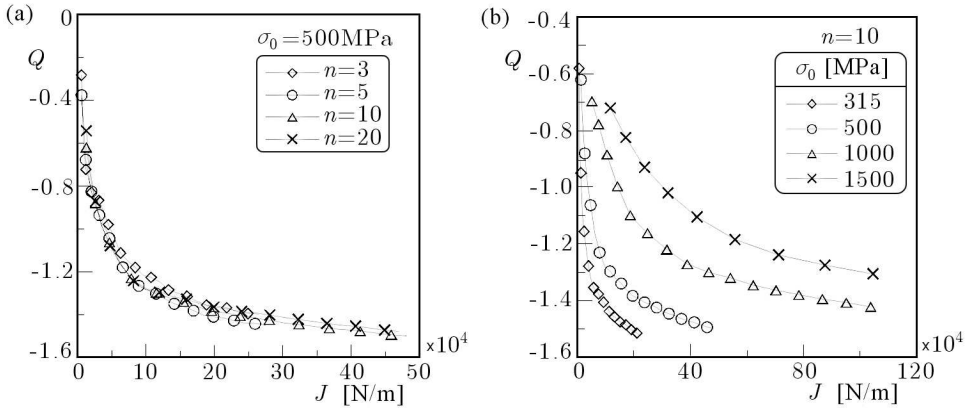


Fig. 7. The influence of the work-hardening exponent (a) and the yield strength (b) on  $Q$ -stress values for CC(T) specimens (own calculation);  $W = 40 \text{ mm}$ ,  $a/W = 0.5$ ,  $\nu = 0.3$ ,  $E = 206000 \text{ MPa}$

for a certain group of materials. The best solution would be a catalogue of  $J$ - $Q$  graphs for materials characterized by various yield strengths and different work-hardening exponents. Such a catalogue should take into consideration the influence of the external load, kind of the specimen (SEN(B) specimen – bending, CCT specimen – tension) and geometry of the specimen, too.

In the next part of this paper, values of the  $Q$ -stress will be determined for various elastic-plastic materials for single edge notched specimens under bending (SEN(B)). All results will be presented in a graphical form  $Q = f(J)$  and  $Q = f(\log[J/(a\sigma_0)])$ . Next, the numerical results will be approximated by closed form formulas.

### 3. Details of numerical analysis

In the numerical analysis, the single edge notched specimens in bending (SEN(B)) were used (Fig. 8). Dimensions of the specimens satisfy the ASTM E 1820-05 standard requirements. Computations were performed for plane strain using small strain option. The relative crack length was  $a/W = \{0.05; 0.20; 0.50; 0.70\}$  where  $a$  is a crack length and the width of specimens  $W$  was equal to 40 mm. The choice of the SEN(B) specimen was intentional, because the SEN(B) specimens are used in the laboratory test in order to determine the critical values of the  $J$ -integral, which may be treated as the fracture toughness, if some conditions are satisfied.

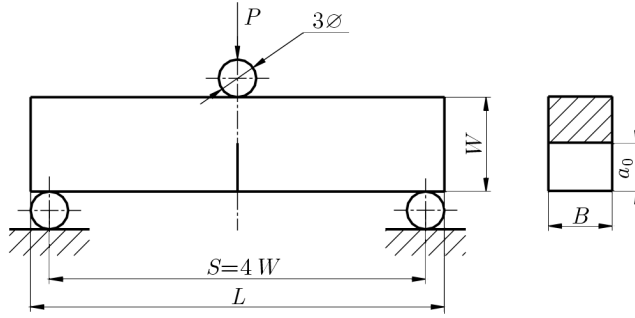


Fig. 8. A single edge notched specimen under bending (SEN(B))

The computations were performed using ADINA SYSTEM 8.3. Due to symmetry, only a half of the specimen was modeled. The finite element mesh was filled with 9-node plane strain elements. The size of the finite elements in the radial direction was decreasing towards the crack tip, while in the angular direction the size of each element was kept constant. The crack tip region was modeled using 36 semicircles. The first of them was 20 times smaller than the last one. It also means that the first finite element behind the crack tip is smaller 2000 times than the width of the specimen. The crack tip was modeled as a quarter of the arc whose radius was equal to  $r_w = 5 \cdot 10^{-6} \text{ m}$  ( $0.000125W$ ). The whole SEN(B) specimen was modeled using 323 finite elements and 1490 nodes. An example of the finite element model for SEN(B) specimen is presented in Figure 9.

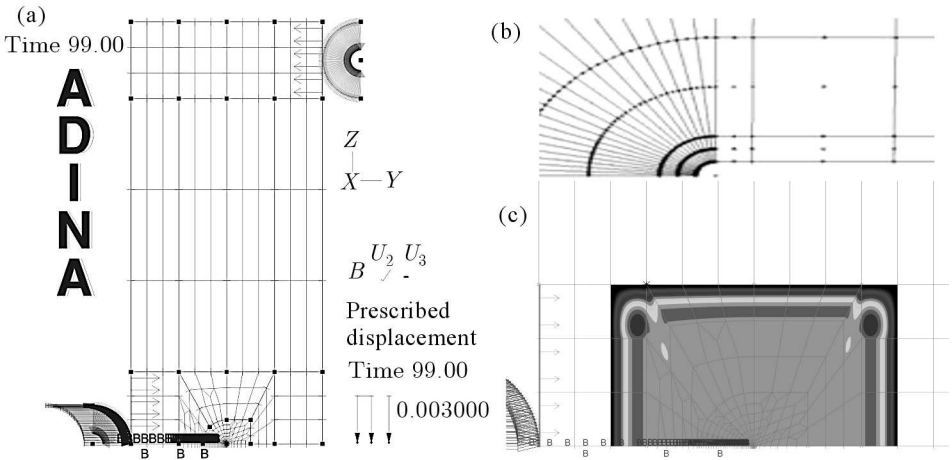


Fig. 9. (a) The finite element model for the SEN(B) specimen; (b) the crack tip model of the SEN(B) specimen; (c) the contour for calculation of the  $J$ -integral

In FEM simulation, the deformation theory of plasticity and the von Mises yield criterion were adopted. In the model, the stress-strain curve was approximated by the relation

$$\frac{\varepsilon}{\varepsilon_0} = \begin{cases} \sigma/\sigma_0 & \text{for } \sigma \leq \sigma_0 \\ \alpha(\sigma/\sigma_0) & \text{for } \sigma > \sigma_0 \end{cases} \quad (3.1)$$

where  $\alpha = 1$ . The tensile properties of materials which were used in the numerical analysis are presented below in Table 1. In FEM analysis, the calculations were done for sixteen materials, which differed by the yield stress and the work hardening exponent.

The  $J$ -integral were calculated using two methods. The first method, called the "virtual shift method", uses the concept of the virtual crack growth to compute the virtual energy change. The second method is based on the  $J$ -integral definition

$$J = \int_C \left[ w dx_2 - \mathbf{t} \left( \frac{\partial \mathbf{u}}{\partial x_1} \right) \right] ds \quad (3.2)$$

where  $w$  is the strain energy density,  $\mathbf{t}$  is the stress vector acting on the contour  $C$  drawn around the crack tip,  $\mathbf{u}$  denotes the displacement vector and  $ds$  is the infinitesimal segment of the contour  $C$ .

In the numerical analysis, 64 SEN(B) specimens were used, which differed by the crack length (different  $a/W$ ) and material properties (different ratio  $\sigma_0/E$  and values of the power exponent  $n$ ).

**Table 1.** Mechanical properties of the materials used in the numerical analysis

$\sigma_0$ [MPa]	$E$ [MPa]	$\nu$	$\varepsilon_0 = \sigma_0/E$	$\alpha$	$n$	$\tilde{\sigma}_{\theta\theta}(\theta = 0)$	$I_n$
315	206000	0.3	0.00153	1	3	1.94	5.51
500			0.00243		5	2.22	5.02
1000			0.00485		10	2.50	4.54
1500			0.00728		20	2.68	4.21

#### 4. Numerical results

The analysis of the obtained results was made in the range  $J/\sigma_0 < r < 6J/\sigma_0$  near the crack tip. The results showed that:

- the  $Q$ -stress decreases if the distance from the crack tip increases (Fig. 10a);

- if the external load increases, the  $Q$ -stress decreases and the difference between the  $Q$ -stress calculated in subsequent measurement points increases (Fig. 10a);
- if the crack length decreases, then the  $Q$ -stress reaches a more negative value for the same  $J$ -integral level (Fig. 10b).

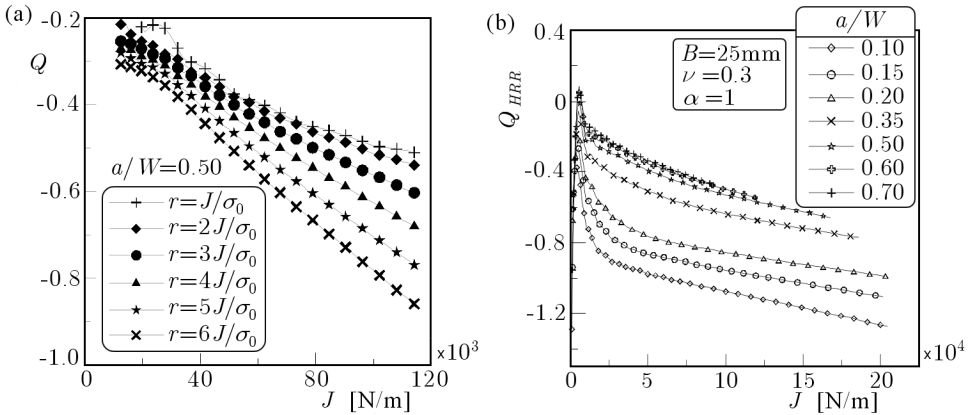


Fig. 10. (a) "The  $J$ - $Q$  family curves" for SEN(B) specimen calculated at six distances  $r$ ; (b) "The  $J$ - $Q$  family curves" for SEN(B) specimen for different crack lengths (plane strain);  $W = 40 \text{ mm}$ ,  $E = 206000 \text{ MPa}$ ,  $\sigma_0 = 315 \text{ MPa}$ ,  $n = 5$

For the sake of the fact that the  $Q$ -parameter, which is used in the fracture criterion and calculated at a distance equal to  $r = 2J/\sigma_0$ , it is necessary to notice that:

- if the yield stress increases, the  $Q$ -parameter increases too, and this applies to all SEN(B) specimens with different crack lengths  $a/W$ ;
- for smaller yield stresses, the  $J$ - $Q$  trajectories shape up much lower and faster changes of the  $Q$ -parameter are observed if the external load increases;
- comparing the  $J$ - $Q$  trajectories for different values of  $\sigma_0/E$ , one observes, that the biggest differences are characterized for materials with small work-hardening exponents ( $n = 3$  – strongly work-hardening materials) and the smallest for materials characterized by a large work-hardening exponent ( $n = 20$  – weakly work-hardening materials); if the crack length increases, this difference somewhat increases too;

- for smaller values of the work-hardening exponent  $n$  (e.g.  $n \leq 5$ ), the  $Q$ -stress becomes more negative;
- if the yield stress decreases, the differences between the  $J$ - $Q$  trajectories characterized for materials described by different work-hardening exponents are bigger;
- for long cracks, the  $Q$ -stress drops more rapidly than for short ones; in the range of small external loads, the  $J$ - $Q$  trajectories for specimens with short cracks shape the lowest; if the external load increases, the  $J$ - $Q$  trajectories for specimens characterized by different  $a/W$  ratios intersect each other; this detail is especially seen for materials characterized by large  $\sigma_0/E$  ratios ( $\sigma_0/E = 0.00485$  and  $\sigma_0/E = 0.00728$ ).

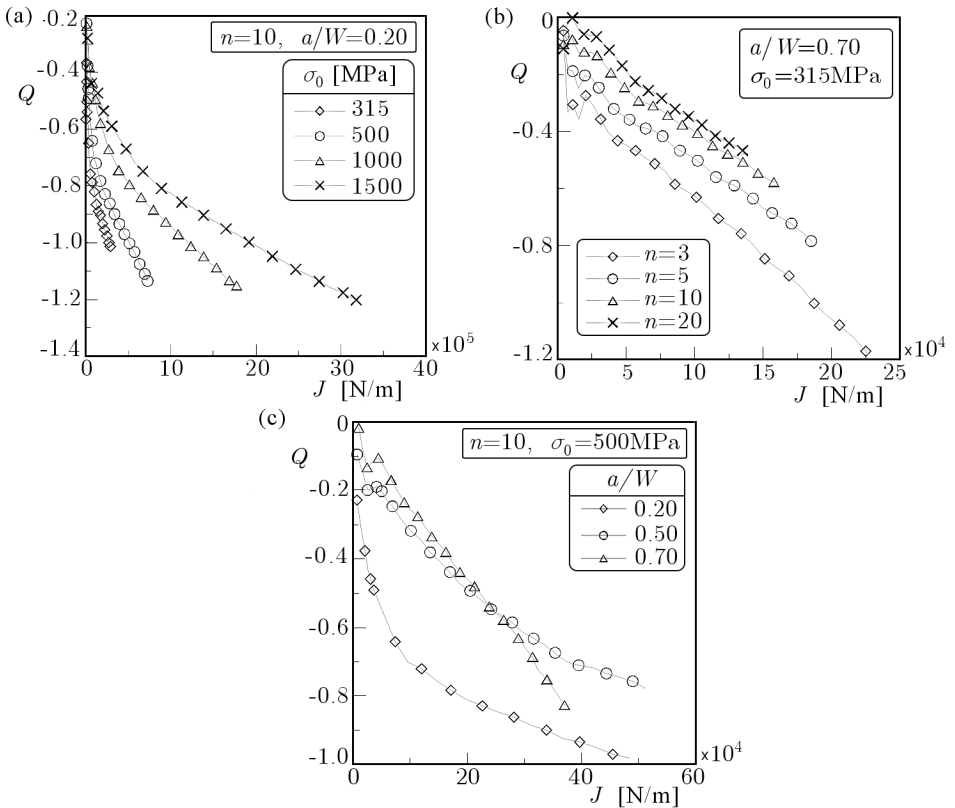


Fig. 11. The influence of: (a) the yield stress on  $J$ - $Q$  trajectories; (b) the work-hardening exponent on  $J$ - $Q$  trajectories; (c) the crack length on  $J$ - $Q$  trajectories for SEN(B) specimens;  $W = 40$  mm,  $E = 206000$  MPa,  $\nu = 0.3$

### 5. Approximation of numerical results

In the literature, mathematic formulas for calculation of the  $Q$ -stress taking into consideration the level of the external load, material properties and geometry of the specimen are not known in most of the cases. The presented in the paper numerical computations provided the reader with the  $J$ - $Q$  catalogue and universal formula (5.1) which allows one to calculate the  $Q$ -stress and take into consideration all parameters influencing the  $Q$ -stress. All results were presented in the  $Q = f(\log[J/(a\sigma_0)])$  graphs. Next, all graphs were approximated by simple mathematical formulas, taking the material properties, external load and specimen geometry into consideration. All the approximations were made for the results obtained at the distance  $r = 2J/\sigma_0$ .

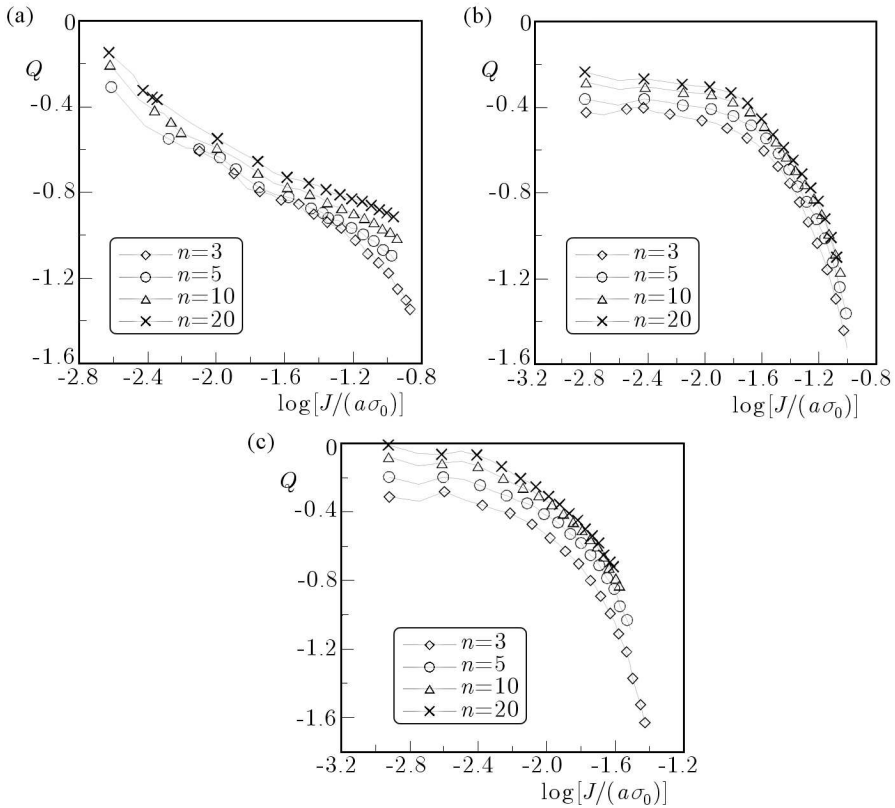


Fig. 12. The influence of the work-hardening exponent on  $Q = f(\log[J/(a\sigma_0)])$  trajectories for SEN(B) specimen ( $W = 40$  mm,  $\nu = 0.3$ ,  $E = 206000$  MPa):  
 (a)  $a/W = 0.20$ ,  $\sigma_0 = 315$  MPa; (b)  $a/W = 0.50$ ,  $\sigma_0 = 1500$  MPa;  
 (c)  $a/W = 0.70$ ,  $\sigma_0 = 500$  MPa

Each obtained trajectory  $Q = f(\log[J/(a\sigma_0)])$  was approximated by a third order polynomial in the form

$$Q(J, a, \sigma_0) = A + B \log \frac{J}{a\sigma_0} + C \left( \log \frac{J}{a\sigma_0} \right)^2 + D \left( \log \frac{J}{a\sigma_0} \right)^3 \quad (5.1)$$

where the  $A, B, C, D$  coefficients depend on the work-hardening exponent  $n$ , yield stress  $\sigma_0$  and crack length  $a/W$ . The rank of fitting formula (5.1) to numerical results for the worst case was equal  $R^2 = 0.990$ . All the coefficients  $A, B, C$  and  $D$  are functions of the work-hardening exponent, and they may be evaluated as

$$A, B, C, D = a_i \left( \ln \frac{1}{n} \right)^3 + b_i \left( \ln \frac{1}{n} \right)^2 + c_i \ln \frac{1}{n} + d_i \quad (5.2)$$

for  $i = 1, \dots, 4$ . In this case, the polynomial was fitted to the numerical results with the accuracy  $R^2 = (0.950-1.000)$ . The obtained coefficients are functions of the yield stress

$$(a_k)^{-1} = A + B \left( \frac{\sigma_0}{E} \right)^3 \quad b_k, c_k, d_k = \frac{A + B \ln \frac{\sigma_0}{E}}{1 + C \ln \frac{\sigma_0}{E}} \quad (5.3)$$

In this case:  $R^2 = (0.980-0.999)$ . For different ratios  $a/W$ , which were not included in the numerical analysis, the coefficients  $a_k, b_k,$  and  $d_k$  may be evaluated using a linear or quadratic approximation. The results of approximation using formulas (5.2) and (5.3) are not published in this paper.

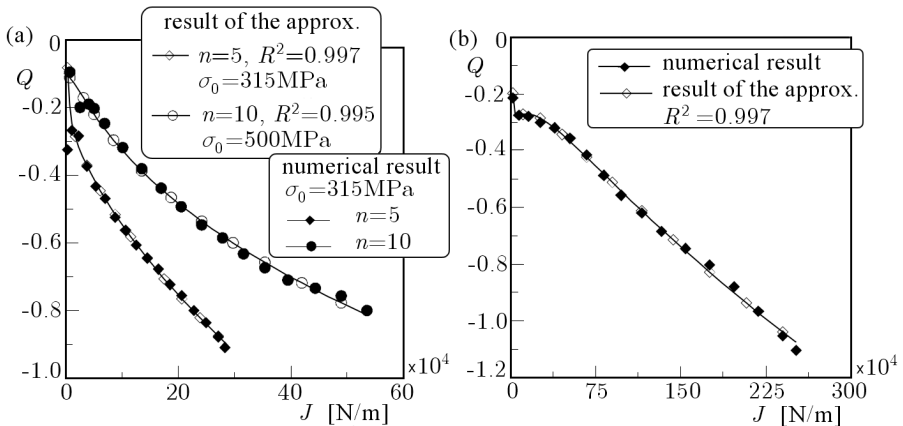


Fig. 13. Comparison of the numerical results and their approximation for  $J$ - $Q$  trajectories for SEN(B) specimens ( $W = 40$  mm,  $a/W = 0.50$ ,  $\nu = 0.3$ ,  $E = 206000$  MPa): (a)  $\sigma_0 = \{315, 500\}$  MPa,  $n = \{5, 10\}$ ; (b)  $\sigma_0 = 1500$  MPa,  $n = 20$

**Table 2.** The coefficients of equation (5.1) for SEN(B) specimen with the crack length  $a/W = 0.05$

$n$	$A$	$B$	$C$	$D$	$R^2$
$\sigma_0 = 315$ MPa			$\sigma_0/E = 0.00153$		
3	-2.91785	-3.54091	-2.49273	-0.65324	0.991
5	-2.49198	-2.41498	-1.44267	-0.30917	0.992
10	-2.13915	-1.87664	-1.27680	-0.34125	0.995
20	-1.66154	-0.70105	-0.70105	-0.07864	0.991
$\sigma_0 = 500$ MPa			$\sigma_0/E = 0.00243$		
3	-2.60090	-3.13553	-2.15010	-0.52678	0.992
5	-2.49503	-2.87049	-1.99305	-0.49037	0.993
10	-1.97971	-1.54825	-0.93643	-0.21897	0.996
20	-1.72018	-0.94662	-0.54570	-0.14425	0.993
$\sigma_0 = 1000$ MPa			$\sigma_0/E = 0.00485$		
3	-1.94316	-1.92526	-1.22276	-0.29192	0.996
5	-1.82250	-1.23157	-0.54551	-0.10531	0.993
10	-1.66826	-0.73998	-0.17472	-0.02837	0.99
20	-1.58000	-0.52871	-0.06815	-0.01236	0.99
$\sigma_0 = 1500$ MPa			$\sigma_0/E = 0.00728$		
3	-1.72349	-1.72747	-1.20275	-0.31647	0.99
5	-1.66343	-0.96989	-0.34106	-0.05949	0.992
10	-1.63267	-0.73176	-0.14559	-0.01541	0.994
20	-1.54170	-0.42219	-0.06755	0.02001	0.992

**Table 3.** The coefficients of equation (5.1) for SEN(B) specimen with the crack length  $a/W = 0.20$

$n$	$A$	$B$	$C$	$D$	$R^2$
$\sigma_0 = 315$ MPa			$\sigma_0/E = 0.00153$		
3	-3.9926	-5.22237	-3.04511	-0.63285	0.998
5	-2.09657	-1.59313	-0.71813	-0.14071	0.995
10	-1.84608	-1.42745	-0.72125	-0.15826	0.998
20	-1.4627	-0.91555	-0.46832	-0.11808	0.999
$\sigma_0 = 500$ MPa			$\sigma_0/E = 0.00243$		
3	-3.1047	-3.42843	-1.70853	-0.30561	0.996
5	-2.34474	-2.10125	-0.94347	-0.16697	0.996
10	-1.69941	-0.98858	-0.28985	-0.04633	0.996

20	-1.28801	-0.28564	0.117374	0.028002	0.993
$\sigma_0 = 1000$ MPa			$\sigma_0/E = 0.00485$		
3	-2.47715	-2.74622	-1.33979	-0.23502	0.996
5	-2.20049	-2.00271	-0.86885	-0.14412	0.997
10	-1.75836	-1.15235	-0.33195	-0.04095	0.998
20	-1.48466	-0.63018	-0.00471	0.021371	0.998
$\sigma_0 = 1500$ MPa			$\sigma_0/E = 0.00728$		
3	-2.33113	-2.45212	-1.19385	-0.20655	0.997
5	-2.15026	-2.03706	-0.91519	-0.15153	0.997
10	-1.87289	-1.46808	-0.54416	-0.07959	0.998
20	-1.33695	-0.67611	-0.10224	0.100436	0.999

**Table 4.** The coefficients of equation (5.1) for SEN(B) specimen with the crack length  $a/W = 0.50$

$n$	$A$	$B$	$C$	$D$	$R^2$
$\sigma_0 = 315$ MPa			$\sigma_0/E = 0.00153$		
3	-5.66457	-5.8778	-2.22163	-0.28531	0.996
5	-3.84704	-3.65795	-1.3143	-0.1674	0.997
10	-2.55848	-1.89569	-0.49284	-0.04543	0.996
20	-1.57524	-0.4334	0.228869	0.067355	0.996
$\sigma_0 = 500$ MPa			$\sigma_0/E = 0.00243$		
3	-6.5155	-7.35971	-2.96692	-0.40099	0.997
5	-4.77859	-5.10234	-1.98063	-0.26344	0.999
10	-2.77426	-2.24203	-0.62248	-0.05688	0.995
20	-1.55052	-0.45388	0.241521	0.076159	0.992
$\sigma_0 = 1000$ MPa			$\sigma_0/E = 0.00485$		
3	-6.13566	-7.07014	-2.88461	-0.38886	0.998
5	-5.33059	-6.13258	-2.51146	-0.34355	0.999
10	-4.25404	-4.57013	-1.74088	-0.22273	0.998
20	-3.76093	-3.813	-1.34863	-0.15913	0.996
$\sigma_0 = 1500$ MPa			$\sigma_0/E = 0.00728$		
3	-6.12	-7.29514	-3.09044	-0.4342	0.996
5	-5.66199	-6.78101	-2.88054	-0.40432	0.998
10	-4.96361	-5.78437	-2.38746	-0.32693	0.998
20	-4.84995	-5.59442	-2.26773	-0.30484	0.997

**Table 5.** The coefficients of equation (5.1) for SEN(B) specimen with the crack length  $a/W = 0.70$

$n$	$A$	$B$	$C$	$D$	$R^2$
$\sigma_0 = 315 \text{ MPa}$			$\sigma_0/E = 0.00153$		
3	-16.3214	-19.749	-8.32577	-1.19313	0.995
5	-7.50229	-7.69853	-2.76341	-0.33713	0.994
10	-4.9541	-4.53575	-1.42694	-0.15244	0.996
20	-3.68993	-2.83418	-0.6574	-0.04004	0.997
$\sigma_0 = 500 \text{ MPa}$			$\sigma_0/E = 0.00243$		
3	-13.8302	-15.5698	-5.98127	-0.7642	0.994
5	-10.1979	-11.2564	-4.2635	-0.54169	0.996
10	-8.4831	-9.10651	-3.34215	-0.41403	0.997
20	-6.88802	-6.8907	-2.32203	-0.26282	0.997
$\sigma_0 = 1000 \text{ MPa}$			$\sigma_0/E = 0.00485$		
3	-12.7605	-14.4196	-5.54031	-0.70258	0.996
5	-10.4778	-11.7531	-4.48806	-0.56847	0.999
10	-9.63775	-10.7617	-4.07619	-0.51445	0.999
20	-9.57785	-10.6301	-3.98443	-0.49841	0.997
$\sigma_0 = 1500 \text{ MPa}$			$\sigma_0/E = 0.00728$		
3	-16.02	-20.18	-8.74	-1.27	0.997
5	-14.99	-18.85	-8.11	-1.16	0.996
10	-12.68	-15.38	-6.34	-0.87	0.998
20	-11.94	-14.17	-5.69	-0.76	0.998

## 6. Conclusions

In the paper, values of the  $Q$ -stress were determined for various elastic-plastic materials for single edge notched specimens undergoing bending (SEN(B)). The influence of the yield strength, the work-hardening exponent and the crack length on the  $Q$ -parameter was tested. The numerical results were approximated by closed form formulas. The most important results are summarized as follows:

- the  $Q$ -stress depends on geometry and the external load; different values of the  $Q$ -stress are obtained for a centrally cracked plate under tension (CC(T)) and different for SEN(B) specimens which are characterized by the same material properties;

- the  $Q$ -parameter is a function of material properties; its value depends on the work-hardening exponent  $n$  and the yield stress  $\sigma_0$ ;
- if the crack length increases, the  $J$ - $Q$  trajectories are characterized by faster changes with the increasing external load.

**Appendix A. Numerical results for the SEN(B) specimen in the plane strain state with the crack length  $a/W = 0.05$**

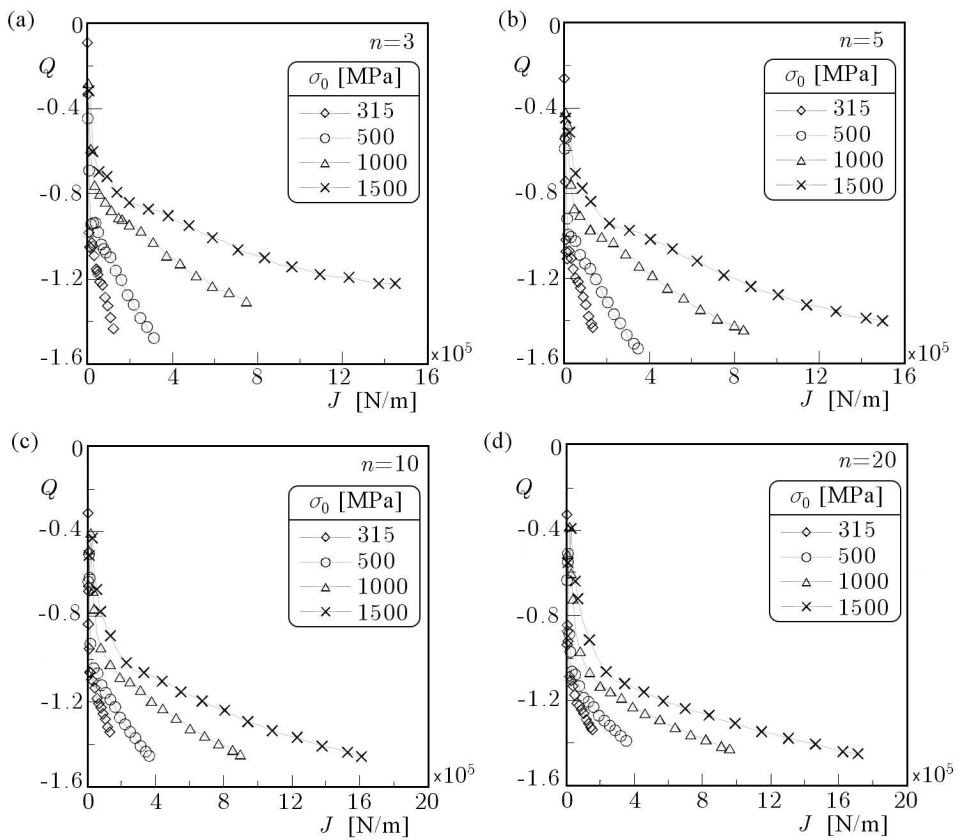


Fig. 14. The influence of the yield stress on  $J$ - $Q$  trajectories for SEN(B) specimens with the crack length  $a/W = 0.05$  for different power exponents in the R-O relationship ( $W = 40$  mm,  $n = 3$ ,  $\nu = 0.3$ ,  $E = 206000$  MPa):

(a)  $n = 3$ ; (b)  $n = 5$ ; (c)  $n = 10$ ; (d)  $n = 20$

**Appendix B. Numerical results for the SEN(B) specimen in the plane strain state with the crack length  $a/W = 0.20$**

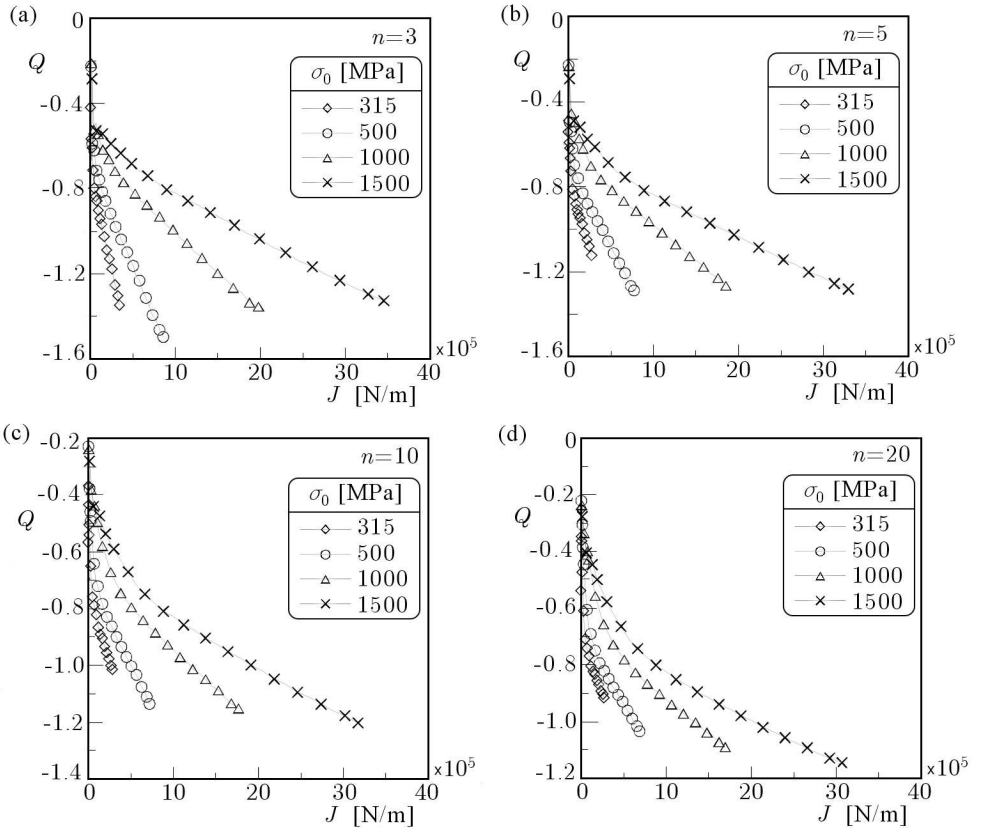


Fig. 15. The influence of the yield stress on  $J$ - $Q$  trajectories for SEN(B) specimens with the crack length  $a/W = 0.20$  for different power exponents in the R-O relationship ( $W = 40$  mm,  $n = 3$ ,  $\nu = 0.3$ ,  $E = 206000$  MPa):  
(a)  $n = 3$ ; (b)  $n = 5$ ; (c)  $n = 10$ ; (d)  $n = 20$

**Appendix C. Numerical results for the SEN(B) specimen in the plane strain state with the crack length  $a/W = 0.50$**

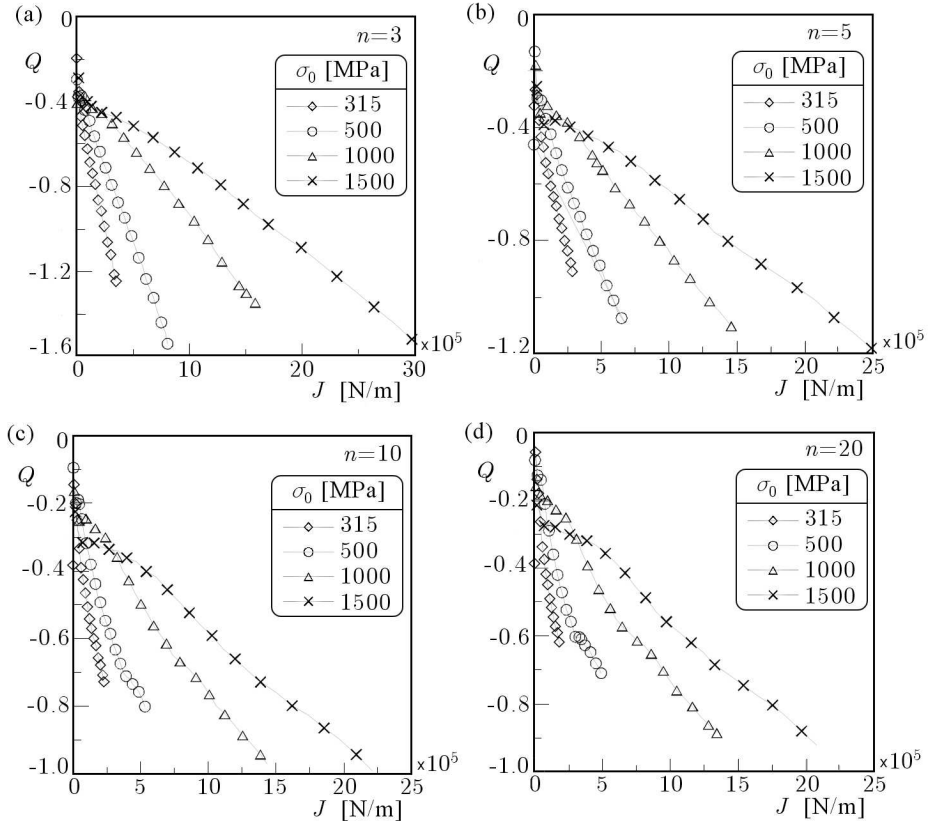


Fig. 16. The influence of the yield stress on  $J$ - $Q$  trajectories for SEN(B) specimens with the crack length  $a/W = 0.50$  for different power exponents in the R-O relationship ( $W = 40$  mm,  $n = 3$ ,  $\nu = 0.3$ ,  $E = 206000$  MPa):

(a)  $n = 3$ ; (b)  $n = 5$ ; (c)  $n = 10$ ; (d)  $n = 20$

**Appendix D. Numerical results for the SEN(B) specimen in the plane strain state with the crack length  $a/W = 0.70$**

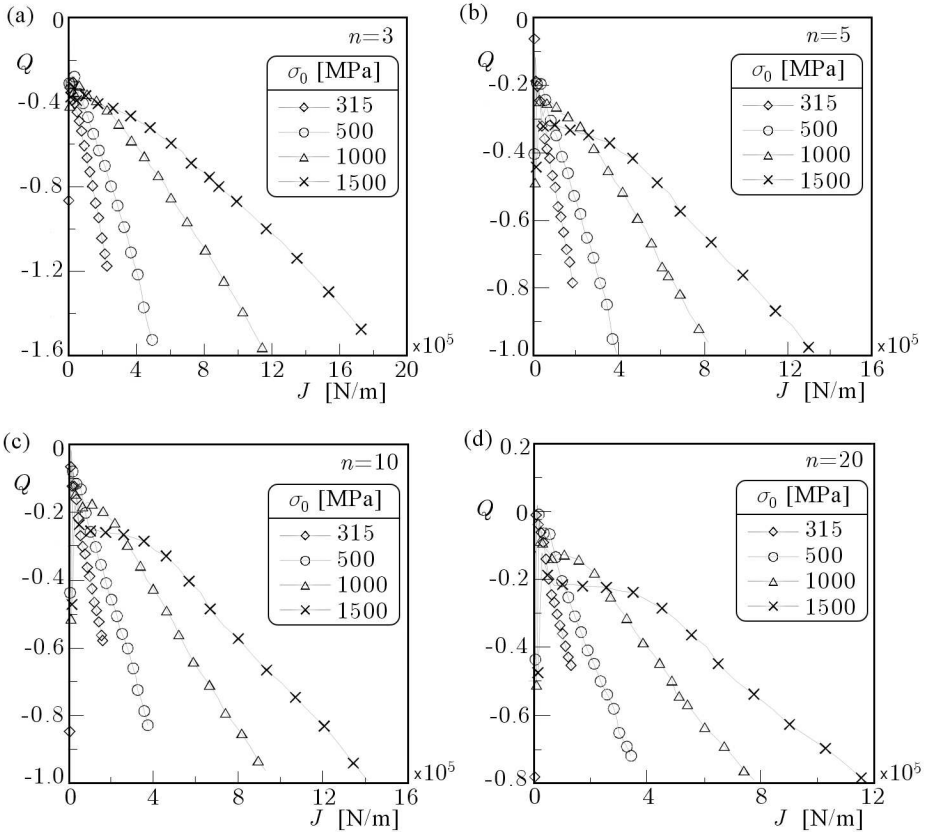


Fig. 17. The influence of the yield stress on  $J$ - $Q$  trajectories for SEN(B) specimens with the crack length  $a/W = 0.70$  for different power exponents in the R-O relationship ( $W = 40$  mm,  $n = 3$ ,  $\nu = 0.3$ ,  $E = 206000$  MPa):  
(a)  $n = 3$ ; (b)  $n = 5$ ; (c)  $n = 10$ ; (d)  $n = 20$

**References**

1. ADINA – Theory and Modeling Guide; Report ARD 04-7; ADINA R&D, Inc.
2. GRABA M., 2007a, The influence of material properties on the  $Q$ -stress value near the crack tip for elastic-plastic materials. Numerical results and their

approximation, *Transcom 2007, Proceedings of the Section 7 – Machines and Equipment. Applied Mechanics*, 59-63

3. GRABA M., 2007b, The influence of material properties on the  $Q$ -stress value near the crack tip for elastic-plastic materials. Theoretical backgrounds, *Transcom 2007, Proceedings of the Section 7 – Machines and Equipment. Applied Mechanics*, 53-57
4. GRABA M., 2007c, Wpływ stałych materiałowych na rozkład naprężeń  $Q$  przed wierzchołkiem pęknięcia w materiałach sprężysto-plastycznych, *IV MSMZMiK – Augustów 2007, materiały konferencyjne*, 109-114
5. GRABA M., GAŁKIEWICZ J., 2006, Algorithm for determination of  $\tilde{\sigma}_{ij}(n, \theta)$ ,  $\tilde{\varepsilon}_{ij}(n, \theta)$ ,  $\tilde{u}_i(n, \theta)$ ,  $d_n(n)$ , and  $I_n(n)$  functions in Hutchinson-Rice-Rosengren solution and its 3D generalization, *Journal of Theoretical and Applied Mechanics*, **44**, 1, 19-30
6. HUTCHINSON J.W., 1968, Singular behaviour at the end of a tensile crack in a hardening material, *Journal of the Mechanics and Physics of Solids*, **16**, 13-31
7. O'DOWD N.P., 1995, Applications of two parameter approaches in elastic-plastic fracture mechanics, *Engineering Fracture Mechanics*, **52**, 3, 445-465
8. O'DOWD N.P., SHIH C.F., 1991, Family of crack-tip fields characterized by a triaxiality parameter – I. Structure of fields, *J. Mech. Phys. Solids*, **39**, 8, 989-1015
9. O'DOWD N.P., SHIH C.F., 1992, Family of crack-tip fields characterized by a triaxiality parameter – II. Fracture applications, *J. Mech. Phys. Solids*, **40**, 5, 939-963
10. RICE J.R., ROSENGREN G.F., 1968, Plane strain deformation near a crack tip in a power-law hardening material, *Journal of the Mechanics and Physics of Solids*, **16**, 1-12
11. SHIH C.F., O'DOWD N.P., KIRK M.T., 1993, A framework for quantifying crack tip constraint, In” *Constraint Effects in Fracture*, ASTM STP 1171, E.M. Hackett, K.-H. Schwalbe, R.H. Dodds, Eds., American Society for Testing and Materials, Philadelphia, 2-20
12. YANG S., CHAO Y.J., SUTTON M.A., 1993, Higher order asymptotic crack tip in a power-law hadening material, *Engineering Fracture Mechanics*, **45**, 1, 1-20

#### *Acknowledgements*

Author gratefully acknowledges support from the Ministry of Science and Higher Education, grant No. N501 264334

## Wpływ stałych materiałowych na rozkład naprężeń $Q$ przed wierzchołkiem pęknięcia w materiałach sprężysto-plastycznych

### Streszczenie

W pracy przedstawione zostaną wartości naprężeń  $Q$  wyznaczone dla szeregu materiałów sprężysto-plastycznych dla próbek trójpunktowo zginanych (SEN(B)), które powszechnie wykorzystuje się do wyznaczania odporności na pękanie w warunkach laboratoryjnych. Omówiony zostanie wpływ granicy plastyczności i wykładnika umocnienia na wartość naprężeń  $Q$ , a także wpływ długości pęknięcia. Wyniki obliczeń numerycznych aproksymowano formułami analitycznymi. Rezultaty pracy stanowią podręczny katalog krzywych  $J$ - $Q$ , możliwy do wykorzystania w praktyce inżynierskiej.

*Manuscript received December 7, 2007; accepted for print January 25, 2008*